Inorg. Chem. **1984**, *23*, 2984-2990

Contribution from the Department of Chemistry,
Harvard University, Cambridge, Massachusetts 02138

Analogues of the $[Fe_4S_4]^+$ Sites of Reduced Ferredoxins: Single-Step Synthesis of the Clusters $[Fe_4S_4(SR)_4]^{3-}$ and Examples of Compressed Tetragonal Core Structures

KARL S. HAGEN, ALAN D. WATSON, and R. H. HOLM*

Received January 23, 1984

Under anaerobic conditions the reaction system $4\ FeCl_2 + 8\ NaSR + 4\ NaSH + 3\ R'_4NCl$ in DMF affords in a single step the reduced cluster $[Fe_4S_4(SR)_4]^{3-}$, isolated as R'_4N^+ salts in yields usually exceeding 60%. Synthesis of clusters with R = Me, Et, CH_2Ph, and *t*-Bu indicates the generality of the method when R = alkyl. The previous synthesis of $[Fe_4S_4(SR)_4]^{3-}$ required chemical reduction of preisolated salts of $[Fe_4S_4(SR)_4]^{2-}$ (R = arene, CH_2Ph). Clusters with R = alkyl are strong reductants ($E_{1/2}(2-/3-) \lesssim -1.3$ V vs. SCE) and thus are extremely sensitive to oxidation. By a ^1H NMR method it is shown that the cluster purity (3– vs. 2–) of the isolated compounds is ≥98%. $(Et_4N)_3[Fe_4S_4(S\text{-}t\text{-}Bu)_4]\cdot MeCN$ crystallizes in monoclinic space group $P2_1/c$ with $a = 23.14$ (3) Å, $b = 11.903$ (5) Å, $c = 24.81$ (4) Å, $\beta = 116.16$ (1)°, and $Z = 4$. $(Me_4N)_3[Fe_4S_4(SEt)_4]$ crystallizes in tetragonal space group $P\bar{4}2_1c$ with $a = b = 12.858$ (2) Å, $c = 11.280$ (2) Å, and $Z = 2$. Both clusters exhibit similar geometries of their $[Fe_4S_4]^+$ cores. In $[Fe_4S_4(S\text{-}t\text{-}Bu)_4]^{3-}$ the core has idealized D_{2d} symmetry with four short (mean 2.297 (6) Å) and eight long (mean 2.330 (7) Å) Fe–S distances roughly parallel and perpendicular, respectively, to the pseudo-$\bar{4}$ axis. $[Fe_4S_4(SEt)_4]^{3-}$ has imposed S_4 symmetry with small deviations from D_{2d} symmetry; four short (2.293 (1) Å) and eight long (mean 2.324 (5) Å) Fe–S distances are approximately parallel and perpendicular, respectively, to the crystallographic $\bar{4}$ axis. These structures are compared with those of other 3– clusters. The compressed tetragonal core structure has not been previously encountered in *reduced* clusters, which do not form a stereoregular set. The compressed tetragonal distortion from cubic core symmetry is a consistent feature of oxidized clusters in which the $[Fe_4S_4]^{2+}$ core is bonded to four identical ligands. In the pair $[Fe_4S_4(S\text{-}t\text{-}Bu)_4]^{2-,3-}$, core distortions are of the same type, and the core volume of the reduced cluster is 2.5% larger than that of the oxidized cluster.

Introduction

Reaction 1 is the electron-transfer couple operative at midpoint potentials near –0.4 V vs. SHE in a large number of ferredoxin (Fd) proteins containing cubane-type Fe_4S_4 clusters.

$$Fd_{ox}([Fe_4S_4]^{2+}) + e^- \rightleftharpoons Fd_{red}([Fe_4S_4]^+) \qquad (1)$$

The synthetic clusters $[Fe_4S_4(SR)_4]^{2-}$ and $[Fe_4S_4(SR)_4]^{3-}$ contain Fe_4S_4 core units that are isoelectronic with Fd_{ox} and Fd_{red}, respectively, and serve as analogues of the redox centers in these proteins.[2-4] The fundamental chemistry of the oxidized clusters has been developed to a substantially greater extent than that of the reduced clusters. This situation derives in large measure from the ease of synthesis of the former from simple reactants, and from higher stability, which permits ready manipulation of terminal ligands and, therewith, cluster properties.[2-4] The only known synthetic route to reduced clusters is by means of reaction 2, in which a preisolated salt of an oxidized cluster is reduced by sodium acenaphthylenide in an aprotic solvent medium under anaerobic conditions.

$$(R'_4N)_2[Fe_4S_4(SR)_4] + R'_4NX + NaC_{12}H_8 \rightarrow (R'_4N)_3[Fe_4S_4(SR)_4] + C_{12}H_8 + NaX \qquad (2)$$

A substantial number of reduced cluster salts has been isolated from this reaction.[5-11] In all cases R = CH_2Ph, Ph, or derivatives of these groups, placing the 2–/3– redox potential at ≥–1.25 V vs. SCE in DMF solution.[12] Earlier attempts to isolate certain R = alkyl cluster salts in analytically pure form failed.[9] These species, for which $E_{1/2}(2-/3-) = -1.29$ V (R = Me) to –1.42 V (R = *t*-Bu) are more strongly reducing than $[Fe_4S_4(SPh)_4]^{3-}$ (–1.04 V) and $[Fe_4S_4(SCH_2Ph)_4]^{3-}$ (–1.25 V), which have been obtained as pure R'_4N^+ salts.

Recently, we have developed a *one-step* synthesis of $[Fe_4S_4(SR)_4]^{3-}$ salts in pure form without the necessity of reducing preisolated oxidized clusters. This method is described here and is shown to produce representative R = alkyl reduced clusters with $E_{1/2}(2-/3-) < -1.3$ V, which have not been previously isolated in high purity. As will be seen, the structures of two newly accessible clusters, $[Fe_4S_4(S\text{-}t\text{-}Bu)_4]^{3-}$ and $[Fe_4S_4(SEt)_4]^{3-}$, emphasize the lack of stereochemical regularity of the odd-electron $[Fe_4S_4]^+$ core found in previous X-ray structural determinations.[2,8,11,13] Indeed, in their particular crystalline environments these species exhibit a compressed tetragonal distortion, which is the stereoregular form of the even-electron $[Fe_4S_4]^{2+}$ cores of oxidized clusters.[2,14,15]

Experimental Section

Preparation of Compounds. Because of the extreme oxygen sensitivity of reduced cluster compounds in the solid and solution states, all operations were performed under a pure dinitrogen or argon atmosphere. Solvents were freshly distilled and degassed. Before use, DMF (Burdick and Jackson, high purity, 0.03% H_2O) and acetonitrile were saturated with oxygen-free argon. Sodium salts of thiolates[16] and NaSH[17] were prepared as described. Anhydrous $FeCl_2$ (99.99%)

---

(1) Sweeney, W. V.; Rabinowitz, J. C. *Annu. Rev. Biochem.* **1980**, *49*, 139.

(2) Berg, J. M.; Holm, R. H. In "Metal Ions in Biology"; Spiro, T. G., Ed.; Wiley: New York, 1982; Vol. 4, Chapter 1.

(3) Holm, R. H.; Ibers, J. A. In "Iron-Sulfur Proteins"; Lovenberg, W., Ed.; Academic Press: New York, 1977; Vol. III, Chapter 7.

(4) Holm, R. H. *Acc. Chem. Res.* **1977**, *10*, 427.

(5) Lane, R. W.; Wedd, A. G.; Gillum, W. O.; Laskowski, E. J.; Holm, R. H.; Frankel, R. B.; Papaefthymiou, G. C. *J. Am. Chem. Soc.* **1977**, *99*, 2350.

(6) Cambray, J.; Lane, R. W.; Wedd, A. G.; Johnson, R. W.; Holm, R. H. *Inorg. Chem.* **1977**, *16*, 2565.

(7) Reynolds, J. G.; Laskowski, E. J.; Holm, R. H. *J. Am. Chem. Soc.* **1978**, *100*, 5315.

(8) Laskowski, E. J.; Frankel, R. B.; Gillum, W. O.; Papaefthymiou, G. C.; Renaud, J.; Ibers, J. A.; Holm, R. H. *J. Am. Chem. Soc.* **1978**, *100*, 5322.

(9) Laskowski, E. J.; Reynolds, J. G.; Frankel, R. B.; Foner, S.; Papaefthymiou, G. C.; Holm, R. H. *J. Am. Chem. Soc.* **1979**, *101*, 6562.

(10) Reynolds, J. G.; Coyle, C. L.; Holm, R. H. *J. Am. Chem. Soc.* **1980**, *102*, 4350.

(11) Stephan, D. W.; Papaefthymiou, G. C.; Frankel, R. B.; Holm, R. H. *Inorg. Chem.* **1983**, *22*, 1550.

(12) DePamphilis, B. V.; Averill, B. A.; Herskovitz, T.; Que, L., Jr.; Holm, R. H. *J. Am. Chem. Soc.* **1974**, *96*, 4159.

(13) Berg, J. M.; Hodgson, K. O.; Holm, R. H. *J. Am. Chem. Soc.* **1979**, *101*, 4586.

(14) Mascharak, P. K.; Hagen, K. S.; Spence, J. T.; Holm, R. H. *Inorg. Chim. Acta* **1983**, *80*, 157.

(15) Cleland, W. E.; Holtman, D. A.; Sabat, M.; Ibers, J. A.; DeFotis, G. C.; Averill, B. A. *J. Am. Chem. Soc.* **1983**, *105*, 6021.

(16) Hagen, K. S.; Holm, R. H. *Inorg. Chem.* **1984**, *23*, 418.

0020-1669/84/1323-2984$01.50/0

was purchased from Cerac. Lower purity commercial samples of this compound gave less satisfactory results.

1. (Et_4N)$_3$[Fe_4S_4(S-*t*-Bu)$_4$]. Solid $FeCl_2$ (5.04 g, 40 mmol) was added to a stirred solution of 8.96 g (80 mmol) of NaS-*t*-Bu in 100 mL of DMF, giving a light red-brown solution and a pale brown suspension. After the reaction mixture was stirred for 30 min, 2.24 g (40 mmol) of NaSH was added. A rapid color change to deep red-brown ensued. The mixture was stirred for 2–3 h, 4.95 g (30 mmol) of Et_4NCl was added, and stirring was continued for 2 h. The solid (mainly NaCl) collected by filtration was washed with 2 × 20 mL of DMF. To the combined filtrate and washings was added slowly with stirring 40 mL of anhydrous ether, causing separation of a black microcrystalline solid. The mixture was kept at −20 °C for 24 h and filtered. The collected solid was washed with 20 mL of ether and dried in vacuo; the crude yield (10.88 g) was nearly quantitative. A portion of this material was recrystallized by slow cooling to ~5 °C of a hot acetonitrile solution after filtration to remove a small amount (~0.5 g) of NaCl. Large black crystals of the acetonitrile monosolvate were obtained and identified by ^{1}H NMR and crystallography (vide infra). This compound desolvated upon storage for ~1 month. The desolvated form was analyzed. Anal. Calcd for $C_{40}H_{96}Fe_4N_3S_8$: C, 43.71; H, 8.80; Fe, 20.33; N, 3.82; S, 23.34. Found: C, 43.67; H, 8.72; Fe, 20.55; N, 3.89; S, 23.20. ^{1}H NMR (CD_3CN): −5.15 ppm (CH_3).

2. (Et_4N)$_3$[Fe_4S_4(SEt)$_4$]. Solid $FeCl_2$ (5.04 g, 40 mmol) was added to a stirred solution of 6.72 g (80 mmol) of NaSEt in ~80 mL of DMF, giving a deep orange-brown solution. After the mixture was stirred for 2 h, 2.24 g (40 mmol) of NaSH was added, causing an immediate color change to deep greenish black. The mixture was stirred for 2 h, 4.97 g (30 mmol) of Et_4NCl was added, and stirring was continued for 3 h. The combined filtrate and washings, obtained as in the previous preparation, were treated with 120 mL of anhydrous ether added slowly with stirring. The resultant thick black oil and mother liquor were maintained at −20 °C for 4 days, during which time the oil changed to flaky black crystals. These were collected, washed with 20 mL of ether, and dried in vacuo, affording 8.56 g (87%) of crude product. This material was recrystallized from 50 mL of acetonitrile by the slow addition of 30 mL of ether and storage of the mixture at −20 °C for 2 days. The solid was collected by filtration, washed with 20 mL of ether, and dried in vacuo; 6.74 g (79%) of pure product as black needles was obtained. Anal. Calcd for $C_{32}H_{80}Fe_4N_3S_8$: C, 38.95; H, 8.17; Fe, 22.64; N, 4.26; S, 25.99. Found: C, 38.89; H, 8.13; Fe, 23.09; N, 4.22; S, 26.05. ^{1}H NMR (CD_3CN): −36.8 (CH_2), −5.41 (CH_3) ppm.

3. (Me_4N)$_3$[Fe_4S_4(SEt)$_4$]·$^1/_2$DMF. a. By Direct Synthesis. The preceding method with Me_4NCl afforded this compound in 20–30% yield as small black needles, which are insoluble in acetonitrile and sparingly soluble in DMF and Me_2SO.

b. From [Fe_4(SEt)$_{10}$]$^{2-}$. To a solution of 1.97 g (2.0 mmol) of (Me_4N)$_2$[Fe_4(SEt)$_{10}$][16] in 20 mL of DMF was added 0.45 g (8.0 mmol) of NaSH. The solution was stirred for 15 min and evacuated to remove EtSH. Addition of 0.79 g (2.0 mmol) of (Me_4N)(BPh_4) caused separation of a microcrystalline solid. The mixture was stirred for 2 h, warmed to ~55 °C, and filtered. The filtrate was cooled to ambient temperature overnight and then to −20 °C. The mother liquor was decanted, and the black crystals were collected, washed with ether, and dried in vacuo; 0.30 g (18%) of product was obtained. A second crop (0.15 g) was obtained by cooling the combined mother liquor and washings to −20 °C, for a total yield of 27%. Anal. Calcd for $C_{20}H_{56}Fe_4N_3S_8$·$^1/_2C_3H_7NO$: C, 30.20; H, 7.01; Fe, 26.12; N, 5.73; S, 30.00. Found: C, 30.34; H, 6.97; Fe, 26.59; N, 5.77; S, 30.32. ^{1}H NMR (Me_2SO-d_6): −36.8 (CH_2), −5.41 (CH_3) ppm.

4. (Et_4N)$_3$[Fe_4S_4(SMe)$_4$]. Solid $FeCl_2$ (2.52 g, 20 mmol) was added to a stirred solution of 2.80 g (40 mmol) of NaSMe in ~75 mL of DMF, giving an intense yellow-brown solution. After the mixture was stirred for 2 h, 1.12 g (20 mmol) of NaSH was added, producing a deep greenish black solution. The mixture was stirred for 2 h, 2.50 g (15 mmol) of Et_4NCl was added, and stirring was continued for 2 h. The combined filtrate and washings (as above) were treated with 30 mL of dry THF added slowly with stirring, and the mixture was cooled at −20 °C for 24 h. After filtration 50 mL of anhydrous ether was added to the filtrate, causing separation of small black crystals. After the mixture was stored at −20 °C for 24 h, the solid was collected by filtration, washed with 20 mL of ether, and dried in vacuo; 2.92 g (63%) of black crystals was obtained. Anal. Calcd for $C_{28}H_{72}Fe_4N_3S_8$: C, 36.13; H, 7.80; Fe, 24.00; N, 4.51; S, 27.56. Found: C, 35.57; H, 7.82; Fe, 23.73; N, 4.68; S, 27.49. ^{1}H NMR (CD_3CN): −42.6 (CH_3) ppm.

Table I. Crystallographic Data for (Et_4N)$_3$[Fe_4S_4(S-*t*-Bu)$_4$]·MeCN (A) and (Me_4N)$_3$[Fe_4S_4(SEt)$_4$] (B)

	A	B
formula	$C_{42}H_{99}Fe_4N_4S_8$	$C_{20}H_{56}Fe_4N_3S_8$
mol wt	1140.18	818.59
a, Å	23.14 (3)	12.858 (2)
b, Å	11.903 (5)	12.858 (2)
c, Å	24.81 (4)	11.280 (2)
β, deg	116.16 (1)	
cryst syst	monoclinic	tetragonal
V, Å^3	6133 (6)	1865 (1)
Z	4	2
d_{calcd}, g/cm^3 [a]	1.23	1.46
space group	$P2_1/c$	$P\bar{4}2_1c$
cryst size, mm	0.14 × 0.26 × 0.40	0.26 × 0.28 × 0.50
radiation	Mo Kα (λ = 0.71069 Å)	
abs coeff, μ, cm^{-1}	11.8	19.7
trans coeff, (min, max)	0.641, 0.751	0.185, 0.212
scan speed, deg/min	2.9–29.3	2.0–29.3
scan range, deg [b]	2.0	2.0
bkgd/scan time ratio	0.25	0.25
data collected	$\pm h, +k, \pm l$ (3.0° ⩽ 2θ ⩽ 47°)	$+h, +k, +l$ (3.0° ⩽ 2θ ⩽ 55°); $-h, -k, -l$ (3.0° ⩽ 2θ ⩽ 30°)
unique data ($I > 3\sigma(I)$)	4854	1265
no. of variables	523	98
agmt among equiv reflcns (R_{merge}) [c]	0.0374	0.0575
goodness of fit [d]	1.68	1.22
R, %	4.9	2.6
R_w, %	4.7	2.7

[a] Experimental densities not determined owing to extreme oxidative instability. [b] Scan range = $x + (2\theta_{K\alpha_2} - 2\theta_{K\alpha_1})$. [c] $R_{merge} = [\Sigma_i N_i \Sigma_{j=1}^{N_i} (\bar{F}_j - F_j)^2 / \Sigma_i (N_i - 1) \Sigma_{j=1}^{N_i} F_j^2]^{1/2}$, where N_i is the number of reflections in a given set, F_j is one member of the set, and $\bar{F}_j$ is the mean. [d] GOF = $[w(|F_o| - |F_c|)^2/(n_o - n_v)]^{1/2}$, where n_o and n_v denote the number of data and variables, respectively.

5. (Et_4N)$_3$[Fe_4S_4(SCH_2Ph)$_4$]. This preparation was performed on half the scale of preparation 4 in 50 mL of DMF. The dark brown reaction mixture was stirred for 2 h, NaSH was added (deep brown-black solution), stirring was continued for 2 h, Et_4NCl was added, and the mixture was stirred for an additional 2 h. The volume of the combined filtrate and washings (as above) was condensed in vacuo to ~30 mL. Anhydrous ether (~25 mL) was added slowly until a microcrystalline solid began to separate. The mixture was maintained at −20 °C for 24 h. The solid was collected by filtration, washed with 20 mL of ether, and dried in vacuo to give 1.90 g of black microcrystals. This material was recrystallized from acetonitrile by addition of 1:1 v/v THF/ether; 1.35 g (71%) of product as small black crystals was obtained. The product was not analyzed but was identified as (Et_4N)$_3$[Fe_4S_4(SCH_2Ph)$_4$] by comparison of its ^{1}H NMR spectrum with that of a sample[7] prepared by reaction 2.[6] ^{1}H NMR (CD_3CN): −35.8 (CH_2), −7.70 (*o*-H), −6.93 (*m*-H), −6.43 (*p*-H) ppm.

Collection and Reduction of X-ray Data. Black needles of (Et_4N)$_3$[Fe_4S_4(S-*t*-Bu)$_4$]·MeCN (A) were obtained by slow cooling of an acetonitrile solution of the isolated compound. Small black needles of (Me_4N)$_3$[Fe_4S_4(SEt)$_4$] (B) were grown by layering ether on top of the DMF reaction mixture of preparation 3b, to which (Me_4N)(BPh_4) was not added. Crystals were sealed under argon in glass capillaries. Diffraction data were collected at ~25 °C on a Nicolet R3m four-circle automated diffractometer equipped with a Mo X-ray tube and a graphite monochromator. Data collection parameters and crystal data are collected in Table I. Orientation matrices and unit cell parameters were obtained from 25 machine-centered reflections (20° ≤ 2θ ≤ 25° for compound A and 30° ≤ 2θ ≤ 35° for compound B). Intensities of 3 check reflections measured every 120 reflections revealed no decay over the duration of data

---

(17) Eibeck, R. E. *Inorg. Synth.* **1963**, *7*, 128.

collection. The SHELXTL programs XTAPE and XEMP were used for data processing and empirical absorption corrections, respectively. For compound A the systematic absences $0k0$ ($k = 2n + 1$) and $h0l$ ($l = 2n + 1$) uniquely define the space group $P2_1/c$ (No. 14). All three axial photographs of compound B displayed mirror symmetry indicating the $4/mmm$ Laue group. The systematic absences hhl ($l = 2n + 1$) and $h00$ ($h = 2n + 1$) uniquely define the primitive space group $P\bar{4}2_1c$ (No. 114).

Structure Solution and Refinement. The SHELXTL program package (Nicolet XRD Corp., Madison, WI) was used throughout. Atomic scattering factors were taken from a standard source.[18] The location of all Fe and S atoms of compound A was obtained by use of the direct-methods program SOLV. All remaining non-hydrogen atoms were located by difference Fourier maps and least-squares refinement. Isotropic refinement converged at $R = 9.0\%$. No disorder was evident. Final refinement included anisotropic thermal descriptions of all non-hydrogen atoms. Fixed contributions for hydrogen atoms at idealized positions (C–H = 0.96 Å) were included but not refined. For compound B a value of $Z = 2$ in space group $P\bar{4}2_1c$ indicates that the anion is situated on a $\bar{4}$ axis. The location of the Fe atom was determined from a Patterson map and was confirmed by direct methods (SOLV), which also revealed the location of the bridging and terminal S atoms. The remaining nonhydrogen atoms were located from difference Fourier maps. The unit cell contents include two anions on $\bar{4}$ axes, two cations also on $\bar{4}$ axes, and four cations on 2-fold axes. Isotropic refinement converged at $R = 7.7\%$ and anisotropic refinement based on the original coordinates at R = 3.8%. The coordinates were inverted after a multiplier of the $\Delta f'$ values was refined to −1, indicating that the polarity of the structure was incorrect. Unreasonable anion S–C (2.03 Å) and C–C (1.23 Å) distances indicated a disorder problem. This was successfully modeled in terms of the two orientations C(1a)–C(2a) and C(1b)–C(2b) (Table II). The thiolate S atom was not disordered. Hydrogen atoms were included as for compound A. Both structures were refined to acceptable R values, which are given in Table I. At this stage the polarity of the structure of compound B was again checked by inverting the coordinates, whereupon the R value increased by 1.0%. Atom coordinates for the anion of compound A and for compound B are collected in Table II.[19]

Other Physical Measurements. ^1H NMR spectra (300 MHz) were determined at ~297 K with a Bruker WM-300 spectrometer. Chemical shifts downfield of Me_4Si reference are designated as negative. Measurements were made under strictly anaerobic conditions. Hydrogen evolution from reaction systems was checked by gas chromatography using equipment described elsewhere.[20]

Results and Discussion

Synthesis. Under strictly anaerobic conditions reaction system 3 affords quaternary ammonium salts of the reduced clusters $[Fe_4S_4(SR)_4]^{3-}$ in yields usually exceeding 60%. The

$$4FeCl_2 + 8NaSR + 4NaSH + 3R'_4NCl \xrightarrow[Ar]{DMF} (R'_4N)_3[Fe_4S_4(SR)_4] \quad (3)$$

4 equiv of NaSR in excess of cluster product composition was added to neutralize protons released from SH^- upon cluster formation. The reaction is rapid and experimentally convenient. Its generality when R = alkyl is indicated by the successful preparation of cluster salts with R = Me, Et, CH_2Ph, and *t*-Bu. Several attempts to prepare the reduced cluster with R = Ph have been unsuccessful, suggesting a limitation of the method when R = arene. However, reduced clusters with such substituents are readily prepared by reaction 2[5-11] and, owing to their less negative potentials, are easily handled under anaerobic conditions. Cluster salts are soluble in dipolar aprotic solvents and are instantly oxidized upon exposure to air. $(Et_4N)_3[Fe_4S_4(S\text{-}t\text{-}Bu)_4]$, on the basis of its 2−/3− potential,[12,14] is the most strongly reducing Fe–S cluster compound yet isolated.

Table II. Atom Coordinates for $[Fe_4S_4(S\text{-}t\text{-}Bu)_4]^{3-}$ (A) and $[Fe_4S_4(SEt)_4]^{3-}$ (B)[a]

atom	x	y	z
		Compound A	
Fe(1)	0.7937 (1)	0.6825 (1)	−0.0318 (1)
Fe(2)	0.7694 (1)	0.5326 (1)	0.0424 (1)
Fe(3)	0.6777 (1)	0.6905 (1)	−0.0229 (1)
Fe(4)	0.7058 (1)	0.5116 (1)	−0.0798 (1)
S(1)	0.6598 (1)	0.5028 (2)	−0.0132 (1)
S(2)	0.6908 (1)	0.6949 (2)	−0.1111 (1)
S(3)	0.8161 (1)	0.4939 (2)	−0.0218 (1)
S(4)	0.7806 (1)	0.7240 (1)	0.0540 (1)
S(5)	0.8700 (1)	0.8041 (2)	−0.0338 (1)
S(6)	0.8185 (1)	0.4197 (2)	0.1260 (1)
S(7)	0.6099 (1)	0.8196 (2)	−0.0117 (1)
S(8)	0.6595 (1)	0.3680 (2)	−0.1470 (1)
C(15)	0.8744 (5)	0.7897 (8)	−0.1056 (4)
C(25)	0.9342 (7)	0.8436 (14)	−0.0997 (6)
C(35)	0.8703 (7)	0.6696 (10)	−0.1239 (5)
C(45)	0.8175 (7)	0.8453 (13)	−0.1546 (5)
C(16)	0.7741 (4)	0.4341 (7)	−0.1720 (3)
C(26)	0.7118 (5)	0.3698 (8)	0.1437 (4)
C(36)	0.7610 (5)	0.5560 (7)	0.1781 (4)
C(46)	0.8170 (5)	0.3832 (10)	0.2341 (4)
C(17)	0.5341 (4)	0.8196 (7)	−0.0810 (4)
C(27)	0.5424 (5)	0.8766 (8)	−0.1304 (4)
C(37)	0.4834 (5)	0.8823 (11)	−0.0693 (5)
C(47)	0.5122 (5)	0.7042 (8)	−0.1005 (5)
C(18)	0.6861 (4)	0.3721 (7)	−0.2070 (3)
C(28)	0.6556 (5)	0.2732 (9)	−0.2471 (4)
C(38)	0.6600 (7)	0.4764 (9)	−0.2437 (4)
C(48)	0.7580 (4)	0.3695 (11)	−0.1802 (4)
		Compound B	
Fe	−0.1037 (1)	0.9723 (1)	0.9128 (1)
S(1)	0.0376 (1)	0.8612 (1)	0.8881 (1)
S(2)	−0.2373 (1)	0.9418 (1)	0.7797 (1)
C(1a)	−0.2620 (7)	0.8008 (6)	0.8001 (9)
C(1b)	−0.2207 (11)	0.7968 (12)	0.7423 (13)
C(2a)	−0.2029 (7)	0.7411 (7)	0.7116 (10)
C(2b)	−0.2534 (11)	0.7399 (10)	0.8534 (14)
N(1)	0.5000	0.5000	1.0000
C(3)	0.5349 (6)	0.5880 (5)	0.9234 (6)
N(2)	0.0000	0.5000	0.9670 (5)
C(4)	0.0091 (6)	0.5922 (4)	0.8966 (6)
C(5)	0.0935 (5)	0.4906 (7)	1.0434 (6)

[a] Estimated standard deviations are in parentheses in this and the following table.

While reaction 3 provides an efficient preparative method of some generality, several important aspects remain to be clarified. In the method $FeCl_2$ and NaSR in the mole ratio 1:2 were first combined in DMF and allowed to react for 0.5–4 h. Deeply colored reaction mixtures resulted, indicating the formation of iron–thiolate species. The occurrence of reaction 4, from which the product was obtained in 27% yield, indicates

$$(Me_4N)_2[Fe_4(SEt)_{10}] + 4NaSH + (Me_4N)(BPh_4) \xrightarrow[Ar]{DMF} (Me_4N)_3[Fe_4S_4(SEt)_4] \quad (4)$$

that the adamantane-like cage complex $[Fe_4(SEt)_{10}]^{2-}$[16] can act as a cluster precursor.[21] Regardless of the nature of such precursors, reaction 3 might have been expected to yield $[Fe_4S_4(SR)_4]^{4-}$ on the basis of oxidation states of the reactants and the anaerobic conditions employed. These clusters have been detected electrochemically at the potentials $E_{1/2}(3-/4-) \lesssim -1.9$ V in DMF.[12,14] They are much stronger reductants, by ~0.7 V at parity of R group, than are the 3− clusters. The most obvious potential oxidant in reaction 3 is SH^-. This matter was examined in the reaction system with R = Et,

---

(18) Cromer, D. T.; Waber, J. T. "International Tables for X-ray Crystallography"; Kynoch Press: Birmingham, 1974.

(19) See paragraph at the end of this article regarding supplementary material available.

(20) Yamamura, T.; Christou, G.; Holm, R. H. *Inorg. Chem.* **1983**, *22*, 939.

(21) The complexes $[Fe_4(SR)_{10}]^{2-}$ have also been shown to be precursors of the oxidized clusters $[Fe_4S_4(SR)_4]^{2-}$ in reactions with elemental sulfur: Hagen, K. S.; Reynolds, J. G.; Holm, R. H. *J. Am. Chem. Soc.* **1981**, *103*, 4054.

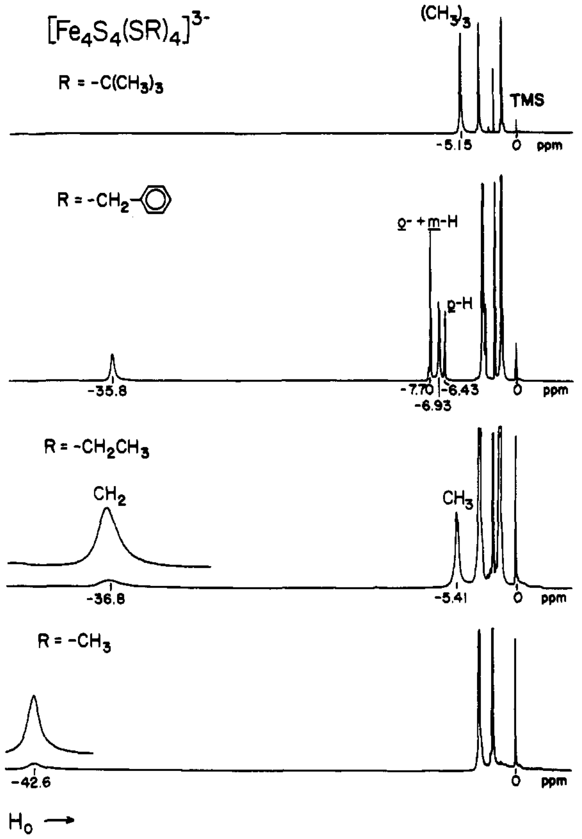

Figure 1. ^1H NMR spectra (300 MHz) of $[Fe_4S_4(SR)_4]^{3-}$ clusters at ~297 K: R = *t*-Bu, CH_2Ph, and Me in CD_3CN solutions; R = Et in Me_2SO-d_6 solution.

containing 1 mmol of $FeCl_2$ and amounts of other reactants as in reaction 3, in 6 mL of DMF. Over a 2-h period after the addition of NaSH, the same reaction time as in preparation 2, no hydrogen was detected by gas chromatography. Experimental conditions were such as to allow detection of the quantity of hydrogen formed under the stoichiometry shown in ref 22. Consequently, the species responsible for partial oxidation of the Fe(II) reactant, required for formation of the $[Fe_4S_4]^+$ core (3 Fe(II) + Fe(III)) of the 3– clusters, remains unidentified. A form of the $[Fe_4S_4]^0$ core sufficiently stable for isolation has been found thus far only in the carbonyl derivative $Fe_4S_4(CO)_{12}$.[23]

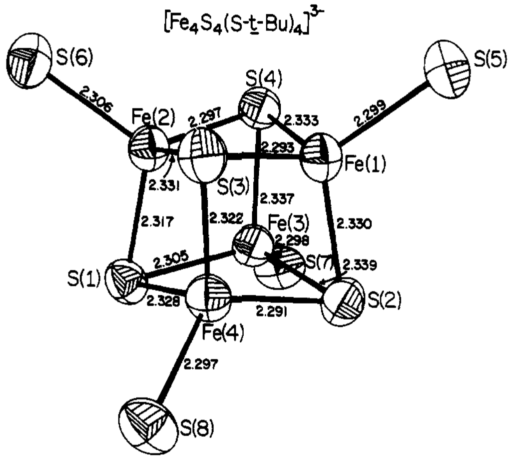

Figure 2. Structure of $[Fe_4S_4(S\text{-}t\text{-}Bu)_4]^{3-}$ showing atom-labeling scheme, 50% probability ellipsoids, and selected interatomic distances. For clarity, the *t*-Bu groups are omitted.

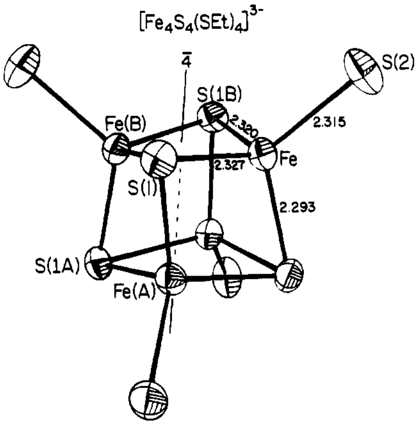

Figure 3. Structure of $[Fe_4S_4(SEt)_4]^{3-}$ showing atom-labeling scheme, 50% probability ellipsoids, selected interatomic distances, and the crystallographically imposed $\bar{4}$ axis. For clarity, the Et groups are omitted.

The $[Fe_4S_4(SR)_4]^{3-}$ clusters are most readily identified and assessed for purity by their ^1H NMR spectra. Four examples are provided in Figure 1. The mixtures $[Fe_4S_4(SR)_4]^{2-,3-}$, at least at >1 mM, exhibit fast-exchange spectra in which chemical shifts are weighted averages of those of 2– and 3– clusters.[10] Electron self-exchange rate constants are ~10^6 M^{-1} s^{-1} at 300 K.[10] Addition of 2-fold molar quantities of sodium acenaphthylenide in THF-d_8 to ~10 mM solutions of $[Fe_4S_4(SR)_4]^{3-}$ prepared from isolated salts caused downfield shifts of ≤0.2 ppm. The latter are taken as limiting values. From the observed shifts of, e.g., $[Fe_4S_4(SCH_2Ph)_4]^{3-}$ in the absence (–35.8 ppm) and presence (–36.0 ppm) of reductant and of $[Fe_4S_4(SCH_2Ph)_4]^{2-}$ (–13.8 ppm), all in CD_3CN solution at 295–297 K, the cluster purity of the product of preparation 5 is calculated to be 99%.[24a] By this procedure the other cluster salts are ≥98% pure. In all cases methylene and methyl shifts are downfield of the values of the corresponding free thiols[25] and the isotropic shifts[24b] are larger than for the corresponding 2– clusters.[7,25] As one comparison, $(\Delta H/H_0)_{iso}$ = –40.6 and –12.8 ppm for $[Fe_4S_4(SMe)_4]^{3-}$ and $[Fe_4S_4(SMe)_4]^{2-}$,[25] respectively, at 294–297 K in CD_3CN solutions. The ~3:1 ratio of shifts is the same as the ratio of magnetic susceptibilities of 3– and 2– clusters at ambient temperature.[7,25] This behavior, together with the negative isotropic shifts, indicates that the latter arise mainly or exclusively from hyperfine contact interactions. Dominant contact shifts, arising from ligand → metal antiparallel spin delocalization, are a consistent property of $[Fe_4S_4(SR)_4]^{2-,3-}$ clusters.[7,25]

Description of Structures. The structures of the anions present in $(Et_4N)_3[Fe_4S_4(S\text{-}t\text{-}Bu)_4]\cdot MeCN$ and $(Me_4N)_3[Fe_4S_4(SEt)_4]$ are shown in Figures 2 and 3, respectively. Stereoviews of the anions are available.[19] Selected interatomic distances and angles are collected in Table III. The crystal structures consist of discrete anions, cations, and solvate molecules. No unusually close contacts of these species were found. Both clusters contain cubane-type $[Fe_4S_4]^+$ cores whose faces are nonplanar Fe_2S_2 rhombs having atom positional deviations of 0.14–0.18 Å from unweighted least-squares planes. The six diagonal planes are nearly perfect, deviations being ≤0.03 Å. The most significant structural features of $[Fe_4S_4(SR)_4]^{2-,3-}$ clusters are those of the Fe_4S_8 portions,

---

[22] $4FeCl_2 + 8NaSR + 4NaSH + 3Et_4NCl \rightarrow (Et_4N)_3[Fe_4S_4(SR)_4] + 11NaCl + 3RSH + NaSR + {}^1/_2H_2$.

[23] Nelson, L. L.; Lo, F. Y.-K.; Rae, A. D.; Dahl, L. F. *J. Organomet. Chem.* **1983**, *225*, 309.

[24] (a) $(\Delta H/H_0)_{obsd} = (1 - N_{3-})(\Delta H/H_0)_{2-} + N_{3-}(\Delta H/H_0)_{3-,lim}$, where N_{3-} is the mol fraction of the 3– cluster. (b) $(\Delta H/H_0)_{iso} = (\Delta H/H_0)_{obsd} - (\Delta H/H_0)_{dia,RSH}$.

[25] Holm, R. H.; Phillips, W. D.; Averill, B. A.; Mayerle, J. J.; Herskovitz, T. *J. Am. Chem. Soc.* **1974**, *96*, 2109.

Table III. Selected Interatomic Distances (Å) and Angles[a] (deg) of $[Fe_4S_4(S\text{-}t\text{-}Bu)_4]^{3-}$ (A) and $[Fe_4S_4(SEt)_4]^{3-}$ (B)

	A	B[b]		A	B[b]
		Fe-S			
Fe(1)-S(3)	2.293 (3)		Fe(4)-S(2)	2.291 (3)	
Fe(2)-S(4)	2.297 (3)	2.293 (1)	mean	2.297 (6)	
Fe(3)-S(1)	2.305 (3)				
Fe(1)-S(2)	2.330 (3)				
Fe(1)-S(4)	2.333 (3)		Fe(3)-S(4)	2.337 (3)	
Fe(2)-S(1)	2.317 (3)		Fe(4)-S(1)	2.328 (3)	2.320 (1)
Fe(2)-S(3)	2.331 (3)		Fe(4)-S(3)	2.322 (3)	2.327 (1)
Fe(3)-S(2)	2.339 (3)		mean	2.330 (7)	2.324 (5)
		Fe-SR			
Fe(1)-S(5)	2.299 (3)		Fe(4)-S(8)	2.297 (3)	2.315 (2)
Fe(2)-S(6)	2.306 (3)		mean	2.300 (4)	
Fe(3)-S(7)	2.298 (3)				
		Fe···Fe			
Fe(1)···Fe(3)	2.790 (3)	2.760 (2)	Fe(2)···Fe(4)	2.736 (2)	
			mean	2.763	
Fe(1)···Fe(2)	2.794 (3)		Fe(3)···Fe(4)	2.786 (3)	2.770 (2)
Fe(1)···Fe(4)	2.749 (2)		mean	2.773 (21)	
Fe(2)···Fe(3)	2.762 (2)		mean (of 6)	2.770 (24)	2.767 (5)
		S···S			
S(1)···S(3)	3.716 (4)		S(2)···S(4)	3.704 (4)	3.699 (2)
			mean	3.710	
S(1)···S(2)	3.631 (4)		S(3)···S(4)	3.616 (4)	3.635 (3)
S(1)···S(4)	3.662 (4)		mean	3.642 (22)	
S(2)···S(3)	3.658 (4)				
		S-C			
S(5)-C(51)	1.838 (13)		S(8)-C(81)	1.844 (11)	1.855 (8)
S(6)-C(61)	1.850 (11)		mean	1.843 (6)	1.89
S(7)-C(71)	1.838 (7)	1.92 (2)			
		C-C			
range (min)	1.47 (2)	1.47 (1)	mean	1.50 (2)	1.49 (2)
range (max)	1.54 (1)	1.51 (2)			
		S-Fe-S			
S(2)-Fe(1)-S(4)	105.2 (1)		S(1)-Fe(4)-S(3)	106.1 (1)	105.4
S(1)-Fe(2)-S(3)	106.2 (1)		mean	105.6	
S(2)-Fe(3)-S(4)	104.8 (1)				
S(2)-Fe(1)-S(3)	104.6 (1)		S(1)-Fe(3)-S(4)	104.2 (1)	
S(3)-Fe(1)-S(4)	102.8 (1)		S(2)-Fe(4)-S(3)	104.9 (1)	103.9
S(1)-Fe(2)-S(4)	105.1 (1)		S(1)-Fe(4)-S(2)	103.6 (1)	103.7
S(3)-Fe(2)-S(4)	102.8 (1)		mean	103.9	103.8
S(1)-Fe(3)-S(2)	102.9 (1)		mean (of 12)	104.5	
		Fe-S-Fe			
Fe(2)-S(1)-Fe(4)	72.2 (1)		Fe(1)-S(4)-Fe(3)	73.4 (1)	72.9
Fe(1)-S(2)-Fe(3)	73.4 (1)		mean	72.8 (2)	
Fe(2)-S(3)-Fe(4)	72.0 (1)				
Fe(2)-S(1)-Fe(3)	73.4 (1)		Fe(1)-S(3)-Fe(4)	73.1 (1)	
Fe(3)-S(1)-Fe(4)	73.9 (1)		Fe(1)-S(4)-Fe(2)	74.2 (1)	73.8
Fe(1)-S(2)-Fe(4)	73.0 (1)		Fe(2)-S(4)-Fe(3)	73.2 (1)	73.6
Fe(3)-S(2)-Fe(4)	74.0 (1)		mean	73.6	73.7
Fe(1)-S(3)-Fe(2)	74.3 (1)		mean (of 12)	73.4	
		RS-Fe-S			
S(5)-Fe(1)-S(3)	118.7 (1)		S(8)-Fe(4)-S(2)	120.7 (1)	118.6 (1)
S(6)-Fe(2)-S(4)	118.8 (1)		mean	119.1	
S(7)-Fe(3)-S(1)	118.2 (1)				
S(5)-Fe(1)-S(2)	116.8 (1)		S(7)-Fe(3)-S(2)	118.4 (1)	
S(5)-Fe(1)-S(4)	107.2 (1)		S(8)-Fe(4)-S(1)	105.6 (1)	110.5 (1)
S(6)-Fe(2)-S(3)	107.8 (1)		S(8)-Fe(4)-S(3)	114.6 (1)	113.4 (1)
S(6)-Fe(2)-S(1)	115.0 (1)		mean	111.5	112.0
S(7)-Fe(3)-S(4)	106.9 (1)		mean (of 12)	114.0	114.2

[a] The standard deviation of the mean is estimated from $\sigma \approx s = [(\Sigma x_i^2 - n\bar{x}^2)/(n-1)]^{1/2}$. [b] Atom-numbering scheme does not apply.

especially of the $[Fe_4S_4]^{2+,+}$ cores.

1. $[Fe_4S_4(S\text{-}t\text{-}Bu)_4]^{3-}$. In a crystal of its Et_4N^+ salt containing one acetonitrile molecule of solvation, no symmetry is imposed on this cluster. The core Fe–S distances divide into sets of four short (2.291 (3)–2.305 (3), 2.297 (6) Å) and eight long (2.317 (3)–2.339 (3), 2.330 (7) Å), with the indicated ranges and mean values. This arrangement provides justification of an idealized $\bar{4}$ symmetry axis that is approximately normal to, and passes through the centers of, faces Fe(1,3)-S(2,4) and Fe(2,4)S(1,3). The short and long bonds are roughly parallel and perpendicular, respectively, to this axis. Under idealized D_{2d} symmetry, other distances and selected angles divide as follows: Fe···Fe and S···S, 2 + 4; S–Fe–S, Fe–S–Fe, and S–Fe–SR, 4 + 8. Distances and angles of the Fe_4S_8 portion are partitioned under this idealized symmetry in Table III. This symmetry is not cleanly reflected by the

Table IV. Structural Comparison of Oxidized and Reduced Clusters

		dist, Å			vol, Å^3			
cluster	axis	Fe···Fe	Fe-S	Fe-SR	Fe_4	S_4	Fe_4S_4	ref
$[Fe_4S_4(S\text{-}t\text{-}Bu)_4]^{2-}$[b]	none	2.76 (2)[a]	4 at 2.252 (8) 8 at 2.315 (5)	2.261 (5)	2.45	5.55	9.68	14
$[Fe_4S_4(S\text{-}t\text{-}Bu)_4]^{2-}$[c]	$\bar{4}$	2.759 (8)	4 at 2.274 (3) 8 at 2.294 (2)	2.254 (3)	2.47	5.53	9.69	14
$[Fe_4S_4(S\text{-}t\text{-}Bu)_4]^{3-}$[c,d]	none	2.77 (2)	4 at 2.297 (6) 8 at 2.330 (7)	2.300 (4)	2.50	5.79	9.93	this work
$[Fe_4S_4(SEt)_4]^{3-}$[e]	$\bar{4}$	2.767 (5)	4 at 2.293 (1) 8 at 2.324 (5)	2.315 (2)	2.49	5.74	9.87	this work
$[Fe_4S_4(SPh)_4]^{3-}$[f,g]	none	2.74 (2)	4 at 2.351 (9) 8 at 2.288 (15)	2.295 (7)	2.43	5.76	9.73	8
$[Fe_4S_4(S\text{-}p\text{-}C_6H_4Br)_4]^{3-}$[c]	2	2.75 (4)	4 at 2.292 (2)[h] 8 at 2.313 (8)	2.297 (15)	2.46	5.70	9.76	11
$[Fe_4S_4(SCH_2Ph)_4]^{3-}$[c]	none	2.76 (2)	6 at 2.302 (4) 6 at 2.332 (5)	2.297 (12)	2.48	5.80	9.86	13

[a] Esd values estimated as in Table III. [b] $(Me_3NCH_2Ph)^+$ salt. [c] Et_4N^+ salt. [d] Acetonitrile monosolvate. [e] Me_4N^+ salt. [f] Et_3MeN^+ salt. [g] Average values of two inequivalent anions. [h] Alternate description: 2 at 2.325 Å, 10 at 2.302 (9) Å.

three types of angles and the Fe···Fe distances. In particular, the large spread of S–Fe–SR angles, external to the core, and irregular Fe_4 subunits are rather frequent features of $[Fe_4S_4(SR)_4]^{2-,3-}$ clusters lacking imposed symmetry but yet meaningfully describable in terms of an idealized Fe–S core skeletal symmetry.[2] The first of these, as in other cases, must arise from packing interactions. The distorted nature of the Fe_4 subunit is evident from the range of Fe···Fe distances. Its nonconformance to the idealized symmetry is further apparent from the ~0.05-Å difference in Fe···Fe distances in the two core faces bisected by the $\bar{4}$ axis.

The nonbonded S···S distances, however, do clearly divide into sets of two long and four short with the mean values 3.71 and 3.64 (2) Å, respectively. The long distances occur in faces bisected by the $\bar{4}$ axis; the short distances are found in the faces parallel to that axis. Thus, the core has (idealized) compressed D_{2d} symmetry. In terms of the differences between the means of long and Fe–S or S···S distances, the extent of compression is 0.03 or 0.07 Å.

2. $[Fe_4S_4(SEt)_4]^{3-}$. As its Et_4N^+ salt the anion is situated on a crystallographically imposed $\bar{4}$ axis. The atoms Fe, S(1), and S(2) (Figure 3) constitute the asymmetric heavy-atom portion of the cluster. Under S_4 cluster symmetry, distances and angles partition as follows: Fe–S, S–Fe–S, Fe–S–Fe, and S–Fe–SR, 4 + 4 + 4; Fe···Fe and S···S, 2 + 4. The metric data in Table III are aligned with corresponding data for $[Fe_4S_4(S\text{-}t\text{-}Bu)_4]^{3-}$ under D_{2d} symmetry. Thus the Fe–S distance of 2.293 (1) Å is associated with the four short Fe–S bonds, and the distances Fe–S(1) = 2.327 (1) Å and Fe–S(1B) = 2.320 (1) Å are correlated with the eight long Fe–S bonds, of the latter cluster.[26] Deviations of $[Fe_4S_4(SEt)_4]^{3-}$ from D_{2d} symmetry are small. This cluster also possesses *compressed* tetragonal symmetry, a structure further emphasized by two long S···S distances of 3.699 (2) Å in the faces bisected by the $\bar{4}$ axis and four short S···S distances of 3.635 (3) Å in faces parallel to this axis. In terms of corresponding mean values of $[Fe_4S_4(S\text{-}t\text{-}Bu)_4]^{3-}$ and unique or mean values of $[Fe_4S_4(SEt)_4]^{3-}$, which for core distances and angles differ by ≤0.015 Å and ≤0.7°, respectively, the two clusters are virtually isostructural.

Core Structural Comparisons. Assembled in Table IV are selected structural data for oxidized and reduced clusters. More extensive listings of oxidized clusters and their structural properties are available elsewhere.[2,14] All species with the $[Fe_4S_4]^{2+}$ core and four identical terminal ligands, whether RS^-,[2,14] Cl^-,[2,27] or PhO^-,[15] exhibit compressed tetragonal core structures. These are of idealized D_{2d} symmetry except for one salt of $[Fe_4S_4(S\text{-}t\text{-}Bu)_4]^{2-}$, where D_{2d} symmetry is imposed. In contrast, the $[Fe_4S_4]^+$ cores of five reduced clusters are not of a stereoregular type. Two inequivalent anions of $[Fe_4S_4(SPh)_4]^{3-}$ contain four long Fe–S bonds parallel to the idealized $\bar{4}$ axis and thus have an *elongated* D_{2d} structure. $[Fe_4S_4(S\text{-}t\text{-}Bu)_4]^{3-}$ and $[Fe_4S_4(SEt)_4]^{3-}$ exhibit the *opposite* tetragonal distortion, which is that found in oxidized clusters. This point is well illustrated by the comparison of $[Fe_4S_4(S\text{-}t\text{-}Bu)_4]^{2-,3-}$. Of the remaining reduced clusters, $[Fe_4S_4(S\text{-}p\text{-}C_6H_4Br)_4]^{3-}$ has an imposed 2-fold axis. Sorting of Fe–S bonds into short and long categories is ambiguous, the two possibilities being 4 short + 8 long or 10 short + 2 long.[11] The 4 + 8 division in Table IV can be idealized to C_{2v} but not D_{2d} symmetry. $[Fe_4S_4(SCH_2Ph)_4]^{3-}$ has a 6 + 6 arrangement that conforms to idealized C_{2v} symmetry. In these descriptions there are four ($[Fe_4S_4(SCH_2Ph)_4]^{3-}$) and two or four ($[Fe_4S_4(S\text{-}p\text{-}C_6H_4Br)_4]^{3-}$) short Fe–S bonds parallel to the 2-fold axis. To this extent these clusters resemble $[Fe_4S_4(S\text{-}t\text{-}Bu)_4]^{3-}$ and $[Fe_4S_4(SEt)_4]^{3-}$. Regardless of the type of distortion, core volumes (calculated from atom coordinates) change relatively little. The largest $[Fe_4S_4]^+$ volume (9.93 Å^3) exceeds the smallest (9.73 Å^3) by only 2.1%; the corresponding value for $[Fe_4S_4]^{2+}$ cores is 2.0%.[14]

In previous investigations of $[Fe_4S_4(SR)_4]^{2-,3-}$ clusters we have provided a substantial body of evidence that the intrinsic core structural change attendant to electron transfer is that in reaction 5.[8,9,11] The compressed tetragonal form of the

$$\underset{\substack{\text{compressed}\\ D_{2d}}}{[Fe_4S_4]^{2+}} + e^- \rightleftharpoons \underset{\substack{\text{elongated}\\ D_{2d}}}{[Fe_4S_4]^{+}} \quad (5)$$

oxidized core has been considered to be the intrinsically stable arrangement on the basis that some seven clusters in eight crystalline environments[2,14,15,27] show this departure from cubic core symmetry. The structures of the same cluster, $[Fe_4S_4(S\text{-}t\text{-}Bu)_4]^{2-}$, in two crystalline forms illustrate this point. Recent structural determinations of the mixed-ligand clusters $[Fe_4S_4(XPh)_2Cl_2]^{2-}$ (X = O, S)[28] have provided the first instances of oxidized cores whose Fe–S and S···S distances do not fall into the compressed tetragonal pattern. In these cases the C_{2v} core symmetry inflicted by the mixed-ligand set pre-

---

(26) Note that in the depictions of Figures 2 and 3, the $\bar{4}$ axes are oriented at ~90°.

(27) Bobrik, M. A.; Hodgson, K. O.; Holm, R. H. *Inorg. Chem.* **1977**, *16*, 1851.

(28) Kanatzidis, M. G.; Baenziger, N. C.; Coucouvanis, D.; Simopoulos, A.; Kostikas, A. *Inorg. Chem.*, in press.

vails. Lacking clear evidence to the contrary, we adhere to the view that the compressed form of $[Fe_4S_4]^{2+}$ cores in identical-ligand environments is the most stable arrangement, but one whose degree of distortion is subject to extrinsic effects of the environment. The different extents of compression of $[Fe_4S_4(S\text{-}t\text{-}Bu)_4]^{2-}$ in two lattices provide a clear case in point. In three Fd_{ox} proteins the cores, bonded to four necessarily inequivalent cysteinate residues, also have the compressed tetragonal structure.[29,30] No structure of a Fd_{red} protein is available.

The proposition that the elongated tetragonal form of the $[Fe_4S_4]^+$ core is the intrinsically stable structure is based on the near-congruence of spectroscopic and magnetic properties of reduced clusters in solution with those of $[Fe_4S_4(SPh)_4]^{3-}$, which are nearly identical in the solid and solution states.[8,9,11] Some eight $[Fe_4S_4(SR)_4]^{3-}$ clusters exhibit this behavior. These include the R = $p\text{-}C_6H_4Br$ and CH_2Ph species, which have nontetragonal structures in the solid state. Solution structures are considered to be less perturbed than those in the solid state and thus to correspond to the most stable configuration. Other R = alkyl clusters, not being previously accessible, were not examined. If the proposal in reaction 5 is to be more generally upheld, the R = Et and *t*-Bu clusters, upon passing from the crystalline to the solution phase, must execute a compressed → elongated tetragonal structural change. This process involves inversion in length of the 4 short + 8 long Fe–S bond sets and is comparable to the structural change in reaction 5 itself. The comparative properties of reduced clusters with R = alkyl, as related to the occurrence of reaction 5, are under investigation.

Acknowledgment. This research was supported by NIH Grant GM 28856. We thank Prof. D. Coucouvanis for a preprint of ref 28 and J. M. Berg for volume calculations and useful discussions.

Registry No. A, 91294-56-3; B, 91294-59-6; $(Et_4N)_3[Fe_4S_4(SEt)_4]$, 91294-58-5; $(Et_4N)_3[Fe_4S_4(SMe)_4]$, 91294-61-0; $(Et_4N)_3[Fe_4S_4(SCH_2Ph)_4]$, 63182-82-1; $(Me_4N)_2[Fe_4(SEt)_{10}]$, 88271-63-0.

Supplementary Material Available: Crystallographic data for $(Et_4N)_3[Fe_4S_4(S\text{-}t\text{-}Bu)_4]\cdot MeCN$ and $(Me_4N)_3[Fe_4S_4(SEt)_4]$: listings of atom coordinates, anisotropic thermal parameters, and calculated hydrogen atom positions and temperature factors, tables of $10|F_o|$ and $10|F_c|$, and stereoviews of the clusters (42 pages). Ordering information is given on any current masthead page.

---

(29) Carter, C. W., Jr. In "Iron-Sulfur Proteins"; Lovenberg, W., Ed.; Academic Press: New York, 1977; Vol. III, Chapter 6.

(30) Stout, C. D. In "Metal Ions in Biology"; Spiro, T. G., Ed.; Wiley: New York, 1982; Vol. 4, Chapter 3.

Contribution from the Laboratory of Analytical Chemistry,
Faculty of Science, Nagoya University, Nagoya, 464 Japan

Enhanced Reactivity of Nickel(II) Complexes Involving Multidentate Ligands in Their Complexation

SHINKICHI YAMADA, TAKATOSHI KIDO, and MOTOHARU TANAKA*

Received September 13, 1983

The formation rates of the 1:1 and 1:2 nickel(II) oxalato (ox^{2-}), glycinato (gly^-), and ethylenediamine (en) complexes with 1,10-phenanthroline have been studied spectrophotometrically by a stopped-flow technique. The rate law is expressed as $d[Ni(phen)^{2+}]/dt = k_{Ni}[Ni^{2+}][phen] + k_{NiA}[NiA][phen] + k_{NiA_2}[NiA_2][phen]$, where phen refers to unprotonated 1,10-phenanthroline and A to a bidentate ligand. The enhanced reactivity of NiA as compared to that of Ni^{2+} ($k_{Ni} = (4.2 \pm 0.2) \times 10^3\ M^{-1}\ s^{-1}$, $k_{Ni(ox)} = (1.8 \pm 0.2) \times 10^4\ M^{-1}\ s^{-1}$, $k_{Ni(gly)} = (1.9 \pm 0.2) \times 10^4\ M^{-1}\ s^{-1}$, and $k_{Ni(en)} = (1.6 \pm 0.2) \times 10^4\ M^{-1}\ s^{-1}$, all at 25 °C and $I = 1.00$ M) is attributable to the labilizing effect of the bound ligand A on the rate of loss of coordinated water molecules at NiA. The labilizing effect of the coordinated aliphatic multidentate ligand is quantitatively accounted for in terms of the electron-donating ability of the coordinated ligand.

From mechanistic considerations on the formation constants of metal complexes,[1,2] it has been shown that, taking into account the statistical factor arising from the number of water molecules available for exchange, the water-exchange rate constant at MA ($k_{MA}{}^{-H_2O}$) is expressed as

$$\log (k_{MA}{}^{-H_2O}/\text{no. of } H_2O \text{ in MA}) = \log (k_M{}^{-H_2O}/\text{no. of } H_2O \text{ in M}) + \gamma E(A) \quad (1)$$

where $E(A)$ refers to the electron-donor constant of the coordinated ligand A and γ is a constant characteristic of the metal ion M. By the use of the $E(A)$ value as given by Edwards,[3] the bound-ligand effect in the complexation kinetics of monodentate ligand complexes of chromium(III),[4] cobalt(II),[4] iron(III),[4] nickel(II),[4-6] oxovanadium(IV),[4] zinc(II),[7] and gallium(III)[8] has been shown to be quantitatively described by eq 1.

For the complexation kinetics involving multidentate ligand complexes, rate constants for the substitution of water molecules in the first coordination sphere of MA, especially of NiA, have been determined for many systems,[9] and it has been observed that a bound ligand exerts a significant influence on the reactivity of nickel(II). For A = aliphatic amine, the increasing lability of the water molecules at NiA with increasing number of nitrogen atoms bound to nickel(II) has been noted.[10,11]

To understand how the bound-ligand effect of nickel(II) complexes can be correlated with the electron-donating ability

---

(1) Tanaka, M. *J. Inorg. Nucl. Chem.* **1973**, *35*, 965–71.

(2) Tanaka, M. *J. Inorg. Nucl. Chem.* **1974**, *36*, 151–61.

(3) Edwards, J. O. *J. Am. Chem. Soc.* **1954**, *76*, 1540–7.

(4) Tanaka, M.; Yamada, S. *J. Chem. Soc., Chem. Commun.* **1976**, 178–9.

(5) Funahashi, S.; Tanaka, M. *Inorg. Chem.* **1969**, *8*, 2159–65.

(6) Funahashi, S.; Tanaka, M. *Inorg. Chem.* **1970**, *9*, 2092–7.

(7) Yamada, S.; Ohsumi, K.; Tanaka, M. *Inorg. Chem.* **1978**, *17*, 2790–4.

(8) Yamada, S.; Tanaka, M., unpublished result.

(9) Margerum, D. W.; Cayley, G. R.; Weatherhburn, D. C.; Pagenkopf, G. K. "Coordination Chemistry, Vol. 2"; Martell, A. E., Ed.; American Chemical Society: Washington, DC, 1978; ACS Monogr. No. 174, Chapter 1.

(10) Margerum, D. W.; Rosen, H. M. *J. Am. Chem. Soc.* **1967**, *89*, 1088–92.

(11) Cobb, M. A.; Hague, D. N. *J. Chem. Soc., Faraday Trans. 1* **1971**, *68*, 932–9.

0020-1669/84/1323-2990$01.50/0